



Immobilization of Tyrosinase on Cu Nanostructures Thin Film as a Potential Tool for Catechol Detection

Ayşe TÜRKHAN^{1*}, Menekşe ŞAKİR², Elif Duygu KAYA³,

¹Iğdır University, Vocational School of Technical Sciences, Department of Chemistry and Chemical Processing Technologies, Iğdır, Türkiye

²ERNAM - Erciyes University Nanotechnology Application and Research Center, Kayseri, Türkiye

³Iğdır University, Faculty of Engineering, Department of Food Engineering, Iğdır, Türkiye

Received: 15 November 2024; Revised: 9 December 2024; Accepted: 19 December 2024

*Corresponding author ayse.turkhan@igdir.edu.tr

Citation: Türkhan, A.; Şakir, M.; Kaya, E.D. *Int. J. Chem. Technol.* 2024, 8(2), 200-207

ABSTRACT

Catechol, a common environmental pollutant and a by-product of many industrial processes, poses a potential threat to the ecosystem and human health. Therefore, the accurate and sensitive detection of catechol is of paramount importance for a wide variety of scientific studies and industrial applications. Immobilized tyrosinase is a valuable tool for facilitating the development of potential phenolic detection applications. This study performed the immobilization of tyrosinase on Cu nanostructures thin film (tyrosinase/Cu NSs-TF) for catechol detection and investigated the optimum working conditions. The successful immobilization process was determined using Fourier-transform infrared spectroscopy (FTIR) and scanning electron microscopy (SEM). The optimum pH and temperature for tyrosinase/Cu NSs-TF were 7.0 and 30°C, respectively. Concerning the reusability of tyrosinase/Cu NSs-TF, it retained over 73% of its activity after the first two replicates and 51.67% after the sixth replicate. When the storage stability of tyrosinase/Cu NSs-TF was investigated at 4°C, it was found that 52.42% of the initial activity was retained until the seventh day. A spectrophotometric method was used for catechol detection. Tyrosinase/Cu NSs-TF displayed a linear response to the concentrations of catechol in the range of 2-90 µM. The limit of detection (LOD) and limit of quantification (LOQ) were calculated to be 7.73 µM and 25.76 µM, respectively. A recovery study was performed with tap water spiked with catechol at concentrations of 30 µM, 60 µM, and 90 µM, yielding recovery rates of 104.44%, 99.58%, and 101.53%, respectively. The results show that tyrosinase/Cu NSs-TF may be a promising approach for catechol detection in water.

Keywords: Catechol detection, Characterization, Cu nanostructures thin film, Immobilization, Tyrosinase.

1. INTRODUCTION

A number of adverse effects on the ecosystem and living systems have accompanied global industrialization. In response to this, interest in detecting and removing hazardous chemicals, such as phenolic compounds, dyes, herbicides, and insecticides, using environmentally friendly methods has increased among researchers.¹⁻² Catechol, one of the hydroxybenzene isomers, is classified as an environmental pollutant by the US Environmental Protection Agency (EPA) and the European Union (EU).³⁻⁴ Catechol is used as a raw material in various industrial processes, including the manufacture of agricultural chemicals, hair dyes, cosmetics, flavorings, pharmaceuticals, textiles, photographic film, antioxidants, and coal conversion processes. Due to the aforementioned industrial

activities, catechol is frequently found in wastewater and can infiltrate groundwater, where it persists and does not degrade easily. Moreover, previous studies have shown that such phenolic compounds can induce DNA damage and carcinogenesis.⁵⁻⁶ Catechol is considered to be toxic to aquatic organisms even at low concentrations.⁷⁻⁸ Consequently, the detection of catechol, which poses a potential threat to the environment and human health, has become a key area of research.⁹ Significant efforts have been made to improve basic and influential methods for the detection of this compound. Commonly used analytical techniques to detect catechol include high-performance liquid chromatography (HPLC),¹⁰ fluorescent probes,¹¹ gas chromatography-mass spectrometry,¹² and electrochemical techniques.¹³ These methods offer high accuracy for catechol detection, but they are encumbered by complex sample pretreatment,

high operating costs, and time-consuming procedures, which restrict their practical applicability.¹⁴ Compared to the aforementioned methods, spectrometric techniques represent a viable alternative for catechol detection, given their inherent simplicity, not requiring specialized expertise, and cost-effectiveness.¹⁵

The utilization of free enzymes is restricted by some factors, including cost, reduced stability, non-reusability, and the inability to recover them after use. Many of these disadvantages of free enzymes can be eliminated by immobilizing enzymes.¹⁶ Enzyme immobilization represents a straightforward and efficacious approach to augmenting the enzyme's activity, stability, and sensitivity, thereby rendering it a valuable tool in industrial processes.¹⁷ Tyrosinase is one of the enzymes used in various contexts across different fields. Tyrosinase catalyzes two reactions in the presence of oxygen: the cresolase activity and the catecholase activity.¹⁸⁻²⁰ Tyrosinase has attracted considerable interest for industrial applications in the bioremediation of phenolic pollutants due to its ability to utilize diverse phenolic compounds as substrates, including 1-3,4-dihydroxyphenylalanine, l-tyrosine, dopamine, phenol, caffeic acid, catechol, p-cresol, p-aminophenol, tyramine, cresol, pyrogallol, 4-butylcatechol, and 4-hydroxyanisole.^{14, 21-24}

Nanomaterials have been researched extensively for various applications in fields, including chemical and biological catalysis, electrocatalysis, photonics, optoelectronics, sensors, and biosensors.²⁵ To obtain highly sensitive results, immobilization of enzyme molecules on a suitable support is necessary. The exceptional properties and technological applicability of various nanostructures have recently made them an attractive potential matrix for enzyme immobilization.^{24, 26-27} The literature has used various nanostructured matrices to immobilize tyrosinase.^{24, 28-29} Nevertheless, there is a constant demand from industry for novel substrates for enzyme immobilization. To the best of our knowledge, the immobilization of tyrosinase on Cu nanostructures thin film has not been previously investigated. Despite the relatively rapid oxidation of copper, it is significantly cheaper than other materials due to its abundance in nature. The in-situ chemical growth of Cu NSs is a cost-effective and labor-saving technique compared to other lithography methods.³⁰ In this study, the tyrosinase enzyme was immobilized on Cu NSs-TF, and catechol was determined by spectrophotometry.

2. MATERIALS AND METHODS

2.1. Chemicals

Poly (ethylene glycol) (PEG, Mw=35.0 kg/mol) and citrate-stabilized Au nanoparticles (Au-NPs) were obtained from Polymer Source Ins. and Ted Pella Ins., respectively. Cetyltrimethylammonium chloride solution ($\text{CH}_3(\text{CH}_2)_{15}\text{N}(\text{Cl})(\text{CH}_3)_3$, 25 wt% in H_2O), tyrosinase

(50 KU), and L (+) ascorbic acid ($\text{C}_6\text{H}_7\text{O}_6\text{Na}$, AA) were purchased from Sigma-Aldrich. Copper (II) acetate monohydrate ($(\text{CH}_3\text{COO})_2\text{Cu}\cdot\text{H}_2\text{O}$), 3-meti-2-benzotiyozolinone (MBTH), dimethylformamide (DMF), and catechol were purchased from Merck.

2.2. Method

2.2.1. Preparation of Cu NSs

2.2.1.1. Organization of the substrate with the PEG brush and linking of Au NPs

As in our previous work,³¹ glass substrates were organized with PEG brushes. To this end, glass substrates cut in 1 cm x 2 cm dimensions were cleaned with distilled water and ethanol, respectively, for 20 minutes in a UV-ozone chamber. Afterward, they were spin-coated with a 2% PEG aqueous solution at 3000 rpm and heated in the glovebox for 2 minutes at 180°C in an argon gas environment. To remove residual PEG chains from the surface, the substrate was washed three times with distilled water for 3 minutes and dried with nitrogen gas. 10 nm Au NPs stabilized with citrate were dropped on it to cover the surface and left in a moist environment for 60 min. Finally, the surface was sonicated with distilled water for 3 minutes and dried with nitrogen gas.

2.2.1.2. Preparation of Cu NSs on Au NPs

To prepare Cu NPs on Au NPs, 20 mg Cu as the metal precursor, 50 mg CTAC solution as the stabilizer, and 40 mg AA as the reducing agent were added to 3 mL of distilled water. The functionalized glass surface was immersed in the solution and stirred in water at 95°C in the dark for 1.5 hours. After the reaction, the surface on which Cu NSs were grown was cleaned with deionized water and then dried with nitrogen gas.³⁰

2.2.1.3. Characterization of Cu NSs and tyrosinase/Cu NSs

The surface morphologies of Cu NSs-TF and tyrosinase/Cu NSs-TF were imaged by scanning electron microscopy (SEM, ZEISS EVO LS 10, 25 keV). The elemental analysis of Cu NSs-TF was performed using energy dispersive X-ray spectroscopy (EDX, Bruker) coupled to SEM. The crystal structure of Cu NSs was analyzed using an X-ray thin film diffractometer (Panalytical Empyrean, Cu $K\alpha$ radiation source:45 kV:40 mA) in the range of 35°-80°.

Before and after enzyme immobilization, FTIR spectrum analysis (PerkinElmer) was conducted at room temperature in the range of 650-4000 cm^{-1} for Cu NSs. The UV-Vis spectrum of tyrosinase/Cu NSs activity was obtained using an Agilent Cary 60 UV-visible spectrophotometer.

2.2.2. Enzyme activity determination

The activity of free and immobilized tyrosinase for the substrate catechol was determined

spectrophotometrically by measuring the increase in absorbance at 500 nm.³² The free tyrosinase reaction mixture was prepared by adding 680 μ L buffer solution (50 mM pH 7.0 phosphate buffer), 100 μ L catechol (100 mM), 100 μ L 3-methyl-2-benzothiazolinone (MBTH) (100 mM), 20 μ L dimethylformamide (DMF), and finally, 100 μ L tyrosinase. The blank contained all components except the enzyme, which was absent. One unit of tyrosinase activity was described as the enzyme quantity inducing an increase in absorbance by 0.001 per minute in a 1 mL reaction mixture.³³

The activity of tyrosinase/Cu NSs-TF was determined by mixing 200 μ L of catechol (100 mM), 200 μ L of MBTH (10 mM), 40 μ L of DMF, 1120 μ L of pH 7.0 phosphate buffer (50 mM), and one piece of tyrosinase/Cu NSs-TF (1 cm x 2 cm), with a total volume of 2000 μ L. The blank contained the entire mixture, with Cu NSs (1 cm x 2 cm) replacing the enzyme. One unit of tyrosinase/Cu NSs-TF activity was determined as the enzyme quantity per centimeter, causing an increase in absorbance of 0.001 per minute in 1 mL of the reaction mixture.^{32, 33-34}

2.2.3. Immobilization of tyrosinase on Cu NSs-TF

1 cm x 2 cm pieces of the Cu NSs matrix were treated in the enzyme tyrosinase solution at 4°C overnight. Subsequently, the samples were washed with buffer three times to remove unbound proteins. Immobilization yield (%) was calculated as follows:

$$\text{Immobilization yield (\%)} = \frac{((X-Y))/X}{X} \cdot 100 \quad (1)$$

In this context, X represents the activity of free tyrosinase prior to immobilization, while Y denotes the total activity of tyrosinase in the filtrate and wash water following immobilization.³⁵

2.2.4. pH effect on the activity of tyrosinase/Cu NSs-TF

To study the effect of pH on the activity of tyrosinase/Cu NSs-TF, separate activity determinations were carried out using sodium acetate buffer (pH 4.0-5.0), phosphate buffer (pH 6.0-7.0), and Tris-HCl buffer (pH 8.0-9.0). The value at which the enzyme exhibited its highest activity was considered to be 100%, and a pH-relative activity graph was plotted.²¹

2.2.5. Temperature effect on the activity of tyrosinase/Cu NSs-TF

The optimum temperature of tyrosinase/Cu NSs-TF was determined by measuring enzyme activity in a water bath within the range of 10-70°C. To that end, reaction mixtures were incubated at the specified temperature in the water bath for 10 minutes, and activity was determined. The value at which the enzyme exhibited its highest activity was considered to be 100%, and a temperature-relative activity (%) graph was plotted.³⁶

2.2.6. Storage stability

The activity of tyrosinase/Cu NSs-TF was monitored at 24-hour intervals by storing the samples at 4°C. The enzyme activity measured on the first day was considered 100%, and the results were evaluated accordingly.³⁷

2.2.7. Reusability

The reusability of tyrosinase/Cu NSs-TF was investigated by performing consecutive activity measurements in the presence of the catechol substrate using the same immobilized enzyme. Tyrosinase/Cu NSs-TF was collected from the medium using tweezers and washed with pH 7.0 phosphate buffer. The enzyme activity determination was repeated.³⁸

2.2.8. Catechol detection

A UV-Vis spectrophotometer was employed for catechol detection. Catechol was prepared at five concentrations, ranging from 2 μ M to 90 μ M. Tyrosinase/Cu NSs-TF (1 cm x 2 cm) was immersed in each concentration of catechol, and the absorbance at 500 nm was recorded at the end of 10 minutes. This process was replicated three times for each concentration, and the resulting averages were calculated. A concentration-absorbance graph was plotted using the obtained data. Linear regression analysis was conducted to calculate the limit of detection (LOD) and limit of quantification (LOQ).³⁹

3. RESULTS and DISCUSSION

3.1. Characterization of Cu NSs

The seed-mediated growth method is quite suitable and useful for achieving an almost homogeneous metallic structure on the surface. Treating the glass surface with UV-ozone not only cleans it but also activates the silanol groups on the surface. Hydroxyl-terminated PEG chains gain mobility during heating and undergo a condensation reaction with the silanol groups on the glass substrate, thereby attaching to the surface. The remaining polymer chains were washed away from the surface. It is well known that citrate-stabilized Au NPs bind to PEG brushes.⁴⁰ The unbound Au NPs on the surface are washed away. As seen in Figure 1a, Au NPs are densely bound to the PEG brushes. The use of Au NPs is crucial because Cu NSs grown directly on the thin-film surface without Au NPs exhibit a more aggressive growth regime and fail to form a homogeneous film surface, as demonstrated in our previous studies. Au NPs act as nucleation centers, facilitating a more controlled and uniform growth of Cu NSs. Thus, their incorporation onto the surface is of significant importance for achieving the desired morphology and uniformity.³⁰ Au NPs, acting as nucleation centers, enabled the in-situ growth of Cu NSs via a wet chemical method. This approach allowed the Cu NSs to adhere stably to the surface, maintaining film integrity during storage without adversely affecting enzymatic activity.

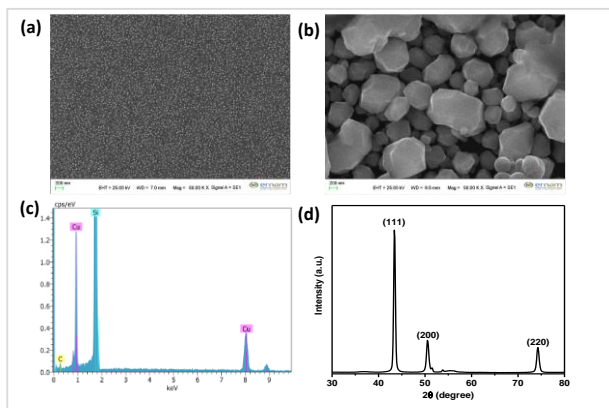


Figure 1. SEM image of (a) 10 nm Au NPs on the PEG brush and (b) Cu NSs grown on Au NPs. (c) EDX analysis of (d) the XRD analysis of Cu NSs.

3.2. Characterization of tyrosinase/Cu NSs-TF

A new matrix, Cu NSs, was prepared for the immobilization of tyrosinase. Previous studies have shown that immobilization occurs between the copper (Cu^{2+}) metal in the matrix and the amino acids in the enzyme's side groups. These include the indole group of tryptophan, the imidazole group of histidine, and the thiol group of cysteine, which are electron-donating amino acid residues. Additionally, metal chelation in conjunction with hydrophobic, electrostatic, and van der Waals interactions are thought to play a role in immobilization.⁴¹⁻⁴⁴ Figure 2 shows the scanning electron microscopy (SEM) images of tyrosinase/Cu NSs-TF. The surface of Cu NSs (Figures 2A, A1) has a granular structure. After immobilization, the granular structure undergoes a transformation, resulting in a new image reminiscent of a mushroom field (Figures 2B, B1). It is clear that the change in the SEM images is a consequence of the enzyme.

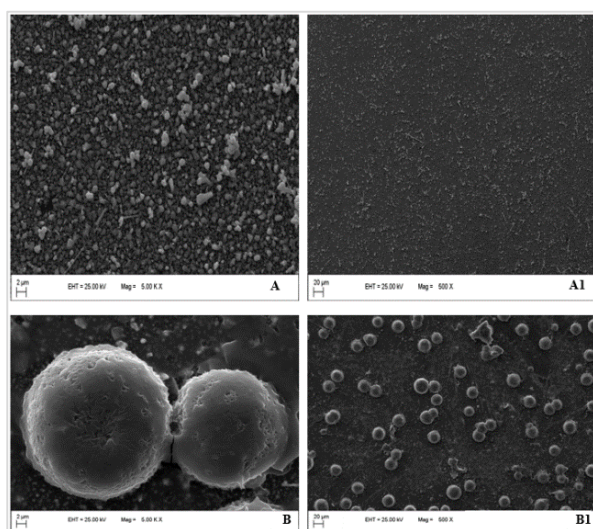


Figure 2. SEM images: (A, A1) Cu NSs-TF and (B, B1) Tyrosinase/Cu NSs-TF.

Figure 3 presents the FTIR analysis results. The FTIR spectra of Cu NSs and tyrosinase/Cu NSs-TF were analysed in the range of $650\text{--}4000\text{ cm}^{-1}$. In the graph, the bands at 1558.027 and 1461.1 cm^{-1} can be attributed to the C=O stretching vibrations of the amide I band and the N-H and C-N stretching vibrations of the amide II band in the protein backbone, respectively. This is due to adding the protein molecule immobilized on Cu NSs.²⁸ The band at 1163 cm^{-1} and 2937 cm^{-1} can be attributed to C-H stretching vibrations.⁴⁵ The results in Figures 2 and 3 demonstrate that immobilization was successful.

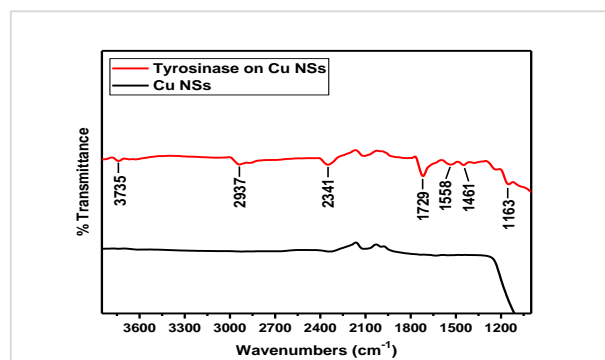


Figure 3. FTIR spectrum of Cu NSs-TF and tyrosinase/Cu NSs-TF.

3.3. Optimum pH

The optimum pH of tyrosinase/Cu NSs-TF was investigated in the presence of catechol as a substrate in the range of pH values from 4.0 to 9.0. The optimum pH for tyrosinase/Cu NSs-TF was 7.0 in phosphate buffer, as shown in Figure 4. The enzyme exhibited high activity in the pH range of 5.0-7.0, with a sharp decrease in activity at pH 4.0, 8.0, and 9.0 (Figure 4). Since the isoelectric point of tyrosinase is between pH 4.7 and 5.0, the charge distribution on the enzyme's side groups is expected to change below this pH value. This change is thought to cause a decrease in enzyme activity at pH 4.0 due to rearrangements in the immobilization bonds.⁴⁶ The decrease in tyrosinase/Cu NSs-TF activity at pH 8.0 and 9.0 can be attributed to two factors: rearrangements in the enzyme's side groups and changes in the matrix structure.⁴⁶⁻⁴⁷ The optimum pH of tyrosinase immobilized on different materials using different methods varies. Similar studies have found the optimum pH to be 6.0 for tyrosinase immobilized on antimony-doped tin oxide thin films (ATO-TFs),⁴⁸ 7.0 for tyrosinase immobilized on glutaraldehyde cross-linked chitosan-clay composite beads,⁴⁹ 7.0 for polyphenol oxidase immobilized on alginate/ZnO nanocomposite materials,⁵⁰ 8.0 for tyrosinase-immobilized thiophene-capped poly(ethylene oxide)/polypyrrole (PEO/PPy) matrices, and 9.0 for tyrosinase-immobilized poly(ethylene oxide)/polypyrrole (CP/PPy) matrices.⁵¹

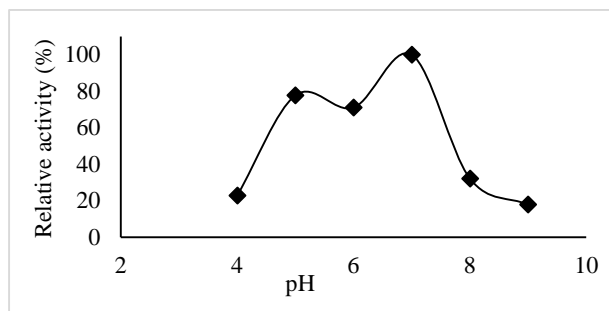


Figure 4. Optimum pH of tyrosinase/Cu NSs-TF.

3.4. Optimum temperature

The optimum temperature for tyrosinase/Cu NSs-TF was determined to be 30°C, within a range of 10-70°C (Figure 5). The Cu NSs matrix was shown to be stable at these temperatures.³⁰ Although the optimum temperature for tyrosinase/Cu NSs-TF was found to be 30°C, the enzyme retained 72.24% of its relative activity at 40°C, 62.42% at 60°C, and 50.21% at 70°C (Figure 5). The ability of tyrosinase/Cu NSs-TF to maintain its activity despite temperature changes can be attributed to immobilization, which better preserves the enzyme's tertiary structure and induces conformational adjustments.⁴⁹ Several studies have shown that the optimum temperature for tyrosinase after immobilization on different matrices varies considerably. Some studies have reported the optimum temperature for immobilized tyrosinase in the range of 25-50°C.^{49, 52-54}

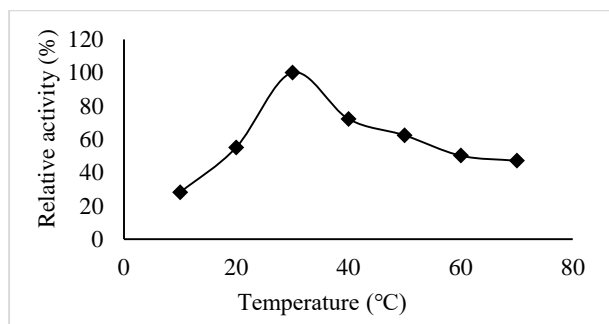


Figure 5. Optimum temperature of tyrosinase/Cu NSs-TF.

3.5. Storage stability and reusability

The stability and reusability of immobilized enzymes are critical factors in any industrial application since they can significantly reduce overall costs.⁵⁵ The storage stability of tyrosinase/Cu NSs-TF was examined at 4°C by measuring enzyme activity at 24-hour intervals for seven days. The storage stability of tyrosinase/Cu NSs-TF decreased to 4.68%, 32.07%, and 47.58% of the initial activity by the end of the second, fourth, and seventh days, respectively (Figure 6). The decline in enzyme activity during storage is believed to be due to keeping the immobilized enzyme in the buffer.⁵⁶ The reusability of tyrosinase/Cu NSs-TF was investigated under optimal conditions. Due to the presence of the matrix on a glass surface, tyrosinase/Cu NSs-TF could be easily recovered

from the reaction medium with tweezers, obviating the need for centrifugation or filtration. Reusability studies were conducted on the immobilized enzyme following washing with buffer. The enzyme retained 77.71% and 73.17% of its activity after the first and second measurements, respectively (Figure 7). In the subsequent measurements, the activity of the immobilized enzyme decreased gradually. After the sixth use, the enzyme retained 51.67% of its original activity. However, by the tenth use, this decreased further, with 61.46% of the original activity being lost. The rapid decline in the initial measurement is thought to be due to removing proteins weakly bound to the surface. The loss of enzyme activity may be attributed to the leaching of weakly bound enzymes, the degradation of the matrix structure upon repeated use, or the binding of the reaction product to the immobilized enzyme, which hinders the enzyme's active site from accessing or binding to the substrate.⁵⁷ The enzyme tyrosinase immobilized on nylon nanofiber membranes demonstrated a considerable decrease in activity following three uses.²³ Polyphenol oxidase immobilized on an alginate/ZnO nanocomposite matrix retained 69% of its activity after ten uses, as reported in reference 50.⁵⁰ immobilized on a sol-gel silica layered matrix retained 30% of its activity after three uses.⁵⁸

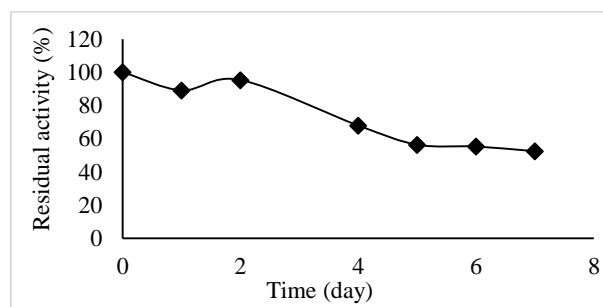


Figure 6. Storage stability of tyrosinase/Cu NSs-TF.

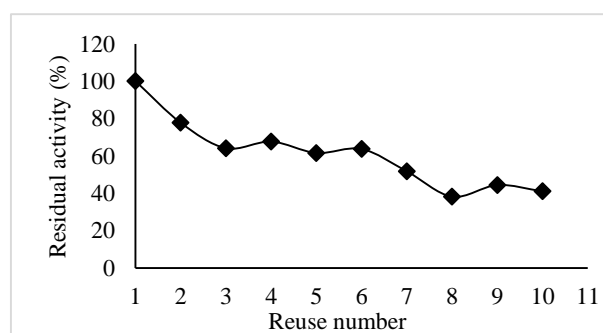


Figure 7. Reusability of tyrosinase/Cu NSs-TF

3.6. Catechol detection

The activity of tyrosinase/Cu NSs-TF was measured for catechol at five concentrations (ranging from 2 to 90 µM) under optimal conditions using a spectrophotometer after a reaction time of 10 minutes. The linear regression analysis of the concentration-absorbance intensity data yielded the equation $y = 0.0008x + 0.0176$, where x is the

concentration of catechol in μM and y is the absorbance intensity. The correlation coefficient (R^2) was 0.9909. LOD and LOQ were calculated using the formulae $\text{LOD} = k \cdot \text{SDa} / b$ ($k = 3$, b is the slope and SDa is the standard deviation of the intercept) and $\text{LOQ} = k \cdot \text{SDa} / b$ ($k = 10$, b is the slope and SDa is the standard deviation of the intercept), respectively. The regression analysis obtained an SDa of 0.00206 and a slope of 0.0008. In the tyrosinase/Cu NSs-TF catechol detection study, LOD and LOQ values were found to be 7.73 μM and 25.76 μM , respectively.

Table 1 compares the limit of detection (LOD) values for catechol detection using the tyrosinase biosensor with those of the tyrosinase/Cu NSs-TF system. As seen in Table 1, the tyrosinase biosensor represents an effective

tool for catechol detection, with voltammetry being a widely employed approach for catechol detection. The spectrophotometer is employed less frequently. The analytical properties of catechol detection with tyrosinase/Cu NSs-TF were found to be similar to those of previously studied biosensors (Table 1).

To evaluate catechol detection in real samples with tyrosinase/Cu NSs-TF, the known concentrations of catechol were prepared in tap water, and it was detected under optimal conditions. Each concentration was repeated three times, and the results are presented as recovery (%) in Table 2. As seen in Table 2, tyrosinase/Cu NSs-TF showed high recovery values even at low concentrations in water sources.

Table 1. Comparison of the calculated LOD and LOQ values for catechol detection between tyrosinase/Cu NSs-TF and some studies in the literature.

Matrix	Analyte	Enzyme	Analytical method	LOD	LOQ	Ref.
$\text{Fe}_3\text{O}_4/\text{Au}$	Catechol	Tyrosinase	Fluorescence spectroscopy	20 μM	-	59
Sol-gel/AuNPs	Catechol	Tyrosinase	Voltammetry	3.0×10^{-6} M	-	60
ITO-silica-PVA	Catechol	Tyrosinase	Voltammetry	10×10^{-6} M	-	61
A sol-gel silica layered matrix	Catechol	Tyrosinase	Spectrophotometry	52 μM	-	58
Agarose-guar gum composite biopolymer matrix	Catechol	Tyrosinase	Voltammetry	6 μM	-	62
MWCNT-MNP/SPE	Catechol	Tyrosinase	Voltammetry	7.61 μM	-	63
Cu NSs-TF	Catechol	Tyrosinase	Spectrophotometry	7.73 μM	25.76 μM	The presented study

Table 2. Catechol detection using tyrosinase/Cu NSs-TF in tap water

Sample No.	Add (μM)	Found ^a (μM)	Recovery (%)
1	30	31,33	104.44
2	60	59,75	99.58
3	90	91.38	101.53

^aAverage of three replicates

4. CONCLUSION

This article reports the first immobilization of tyrosinase onto a Cu NSs matrix. The FTIR and SEM analyses confirmed the successful immobilization of tyrosinase onto Cu NSs. Optimal working conditions for tyrosinase/Cu NSs-TF were determined using UV-Vis spectrophotometry. Due to its thin film structure, tyrosinase/Cu NSs-TF can be easily removed from the reaction medium using tweezers, providing the opportunity to halt the biochemical reaction at any moment. The suitability of tyrosinase/Cu NSs-TF for catechol detection was evaluated by testing it at various concentrations in tap water. The results demonstrated that tyrosinase/Cu NSs-TF is a viable tool for catechol detection, with LOD, LOQ, and recovery % meeting the required standards.

Acknowledgement

The authors would like to thank Iğdır University (BAP, Project No: TBY0820A26) for their financial support.

Conflict of interest:

The authors state no conflict of interest.

REFERENCES

- Koçak, ÇÇ.; Koçak S. *Electroanalysis*. **2020**, 32 (2) 358–366.
- Barveen, NR.; Wang, TJ.; Chang, YH.; Rajakumaran, R. *Mater Sci Eng B*. **2022**, 282, 115753.
- Saleh-Ahammad AJ.; Sarker S.; Aminur Rahman M.; Lee JJ. *Electroanalysis*. **2010**, 22(6), 694–700.

4. Karim-Nezhad, G.; Moghaddam, MH.; Khorablou, Z.; Dorraji, PS.; *J Electrochem Soc.* **2017**, 164(6), B193.
5. Lee, BL.; Ong, HY.; Shi, CY.; Ong, CN. *J Chromatogr B Biomed Sci Appl.* **1993**, 619(2), 259–266.
6. Suvina, V.; Kokulnathan, T.; Wang, TJ.; Balakrishna, RG. *Microchim Acta.* **2020**, 187(3), 1-7.
7. Berno, E.; Pereira-Marcondes, DF.; Ricci Gamalero, S.; Eandi, M. *Ecotoxicol Environ Saf.* **2004**, n57 (2), 118–122.
8. Chandran, M.; Aswathy, E.; Shamna, I.; Vinoba, M.; Kottappara, R.; Bhagiyalakshmi, M. *Mater Today Proc.* **2021**, 46, 3136–3143.
9. Qu, J.; Lou, T.; Wang, Y.; Dong, Y.; Xing, H. *Anal Lett.* **2015**, 48(12), 1842–1853.
10. Petrásková, L.; Káňová, K.; Brodsky, K. *Int J Mol Sci.* **2022**, 23(10), 5743.
11. Wang, B.; Chen, Y.; Wu, Y.; Weng, B.; Liu, Y.; Lu, Z.; Li, CM.; Yu, C. *Biosens Bioelectron.* **2016**, 8, 23–30.
12. Lourenço, ELB.; Ferreira, A.; Pinto, E.; Yonamine, M.; Farsky, SHP. *Chromatographia.* **2006**, 63(3–4), 175–179.
13. Unnikrishnan, B.; Ru, PL.; Chen, SM. *Sensors Actuators B Chem.* **2012**, 169, 235–242.
14. Li, YX.; Sun, Y.; Bai, J.; Chen, SY.; Jia, X.; Huang, H.; Dong, J. *Chinese J Anal Chem.* **2023**, 51(2), 100162.
15. Wang, H.; Wang, J.; Wang, J.; Zhu, R.; Shen, Y.; Xu, Q.; Hu, X. *Sensors Actuators B Chem.* **2017**, 247, 146–154.
16. Gür, B.; Ayhan, ME.; Türkhan, A.; Gür, F.; Kaya, ED. *Colloids Surfaces A Physicochem Eng Asp.* **2019**, 562, 179-185.
17. Liang, S.; Wu, XL.; Xiong, J.; Zong, MH.; Lou, WY. *Coord Chem Rev.* **2020**, 406, 213149.
18. Zawistowskib, J.; Biliaderis, CG.; Eskin, NAM. 1991. Polyphenol oxidase. *Oxidative Enzym foods.* **1991**, 217–273.
19. Martinez, MV.; Whitaker, JR. *Trends Food Sci Technol.* **1995**, 6(6), 195–200.
20. Faccio, G.; Kruus, K.; Saloheimo, M.; Thöny-Meyer, L. *Process Biochem.* **2012**, 47(12), 1749–1760.
21. Colak, A.; Özen, A.; Dincer, B.; Güner, S.; Ayaz, FA. *Food Chem.* **2005**, 90(4), 801–807.
22. Han, E.; Yang, Y.; He, Z.; Cai, J.; Zhang, X.; Dong, X. *Anal Biochem.* **2015**, 486, 102–106.
23. Harir, M.; Bellahcene, M.; Baratto, MC.; Pollini, S.; Rossolini, GM.; Trabalzini, L.; Fatarella, E.; Pogni, R. *J Biotechnol.* **2018**, 265, 54–64.
24. Wu, L.; Yan, H.; Wang, J.; Liu, G.; Xie, W. *J Electrochem Soc.* **2019**, 166(8), B562–B568.
25. Kazemi, SH.; Khajeh, K. *J Iran Chem Soc.* **2011**, 8, 17–19.
26. An, J.; Li, G.; Zhang, Y.; Zhang, T.; Liu, X.; Gao, F.; Peng, M.; He, Y.; Fan, H. *Catalysts.* **2020**, 10(3), 338.
27. Garnica-Romo, MG.; Romero-Arcos, M.; Martínez-Flores, HE. *Mater Res Express.* **2022**, 9, 095005.
28. Gu, BX.; Xu, CX.; Zhu, GP.; Liu, SQ.; Chen, LY.; Li, XS. *J Phys Chem B.* **2009**, 113(1), 377–381.
29. Wu, L.; Deng, D.; Jin, J.; Lu, X.; Chen, J. *Biosens Bioelectron.* **2012**, 35(1), 193–199.
30. Sakir, M.; Yilmaz, E.; Onses, MS. *Microchem J.* **2020**, 154, 104628.
31. Sakir, M.; Pekdemir, S.; Karatay, A.; Küçüköz, B.; Ipekci, HH.; Elmali, A.; Demirel, G.; Onses, MS. *ACS Appl Mater Interfaces.* **2017**, 9(45), 39795–39803.
32. Espín, JC.; Morales M.; Varón, R.; Tudela, J.; García-Cánovas, F. *Journal of Food Science.* **1996**, 61(6), 1177–1182.
33. Galeazzi, MAM.; Sgarbieri, VC.; Constantinides, SM. *J Food Sci.* **1981**, 46(1), 150–155.
34. Türkhan, A.; Faiz, O.; Kaya, ED.; Kocyiğit, A. *Fresenius Environ Bull.* **2018**, 27, 4844–4856.
35. Hou, C.; Wang, Y.; Zhu, H.; Wei, H. *Chem Eng J.* **2016**, 283, 397–403.
36. Kolcuoğlu, Y. *Process Biochem.* **2012**, 47(12), 2449–2454.
37. Arica, MY.; Bayramoğlu, G.; Biçak, N. *Process Biochem.* **2004**, 39(12), 2007–2017.
38. Yavaşer, R.; Aktaş-Uygun, D.; Karagözler AA. *Catal Lett.* **2023**, 153(5), 1265-1277.
39. Önal, A.; Sagirli, O. *Spectrochim Acta A.* **2009**, 72(1), 68-71.

40. Pekdemir, S.; Torun, I.; Sakir, M.; Ruzi, M.; Rogers, JA.; Onses, MS. *ACS nano*. **2020**, 14(7), 8276-8286.
41. Wang, F., Guo, C.; Liu, HZ.; Liu, CZ. *J Chem Technol Biotechnol*. **2008**, 83(1), 97-104.
42. Denizli, A.; Yavuz, H.; Garipcan, B.; Arica, MY. *J Appl Polym Sci*. **2000**, 76(2), 115-124.
43. Wang, Q.; Cui, J.; Li, G.; Zhang, J.; Huang, F.; Wei, Q. *Polymers (Basel)*. **2014**, 6(9), 2357-2370.
44. Gu, YJ.; Zhu, ML.; Li, YL.; Xiong, CH. *Int J Biol Macromol*. **2018**, 112, 1175-1182.
45. John-Kennedy, L.; Selvi, PK.; Padmanabhan, A.; Hema, KN.; Sekaran, G. *Chemosphere*. **2007**,69(2),262-270.
46. Abdollahi, K.; Yazdani, F.; Panahi, R. *Int J Biol Macromol*. **2017**, 94, 396-405.
47. Amjad, R.; Mubeen, B.; Ali, SS.; Imam, SS.; Alshehri, S.; Ghoneim, MM, Alzarea, SI.; Rasool, R.; Ullah, I.; Nadeem, MS.; Kazmi, I. *Polymers*. **2021**, 13(24), 4364.
48. Türkhan, A.; Kaya, ED.; Koçyiğit, A. *Appl Biochem Biotech* **2020**, 192, 432-442.
49. Dinçer, A.; Becerik, S.; Aydemir, T. *Int J Biol Macromol*. **2012**, 50(3), 815-820.
50. Almulaiky, YQ.; Almaghrabi, O. *Catal Lett*. **2022**, 152(10), 3089-3099.
51. Yildiz, HB.; Kiralp, S.; Toppare, L.; Yagci, Y. *Reac Funct Polym*. **2005**, 63(2), 155-161.
52. Camurlu, P.; Kayahan, SK.; Toppare, L. *J Macromol Sci Part A Pure Appl Chem*. **2008**, 45(12), 1009-1014.
53. Uzunoğlu, SB.; Uzunoğlu, T.; Koçsuz, S. *Cell Mol Biol* **2021**, 67(2), 50-55.
54. Zhao, C.; Sha, Y.; Zhuang, W.; Rao, Y.; Zhang, J.; Wu, J.; Shen, T.; Tan, Z.; Zhu, C.; Zhang, H.; Ying, H *Process Biochem*. **2023**, 131, 144-153.
55. Eş, I.; Vieira, JDG.; Amaral, AC. *Appl Microbial Biot*. **2015**, 99, 2065-2082.
56. Şahin, F.; Demirel, G.; Tümtürk, H. *Int l J Biol Macromol*. **2005**, 37(3), 148-153.
57. Lai, YC.; Lin, SC. *A Process Bioche*. **2005**, 40(3-4), 1167-1174.
58. Leboukh, S.; Gouzi, H.; Coradin, T.; Yahi H. *J of Sol-Gel Sci Techn*. **2018**, 86, 675-681.
59. Arkan, E., Karami, C.; Rafipur, R. *JBIC Journal of Biological Inorganic Chemistry*. **2019**, 24, 961-969.
60. Singh, S.; Jain, DVS.; Singla, ML. *Sensor Actuat B-Chem*. **2013**, 182, 161-169.
61. Oriero, DA.; Gyan, IO.; Bolshaw, BW.; Cheng, IF.; Aston, DE. *Microchem J*. **2015**, 118, 166-175.
62. Tembe, S.; Inamdar, S.; Haram, S.; Karve, M.; D'Souza, SF. *J Biotechnol*. **2007**, 128(1), 80-85.
63. Pérez-López, B.; Merkoçi, A. *Adv Funct Mater*. **2011**, 21(2), 255-260.